Dyes and Pigments 84 (2009) 140–147

Contents lists available at ScienceDirect

Dyes and Pigments

journal homepage: www.elsevier.com/locate/dyepig

The synthesis and photodynamic properties of meso-substituted, cationic porphyrin derivatives in HeLa cells

Cheng-Liang Peng [a], Ping-Shan Lai [b], Cheng-Chung Chang [b], Pei-Jen Lou [c], Ming-Jium Shieh [a,d,*]

[a] Institute of Biomedical Engineering, College of Medicine and College of Engineering, National Taiwan University, No. 1, Section 1, Jen-Ai Road, Taipei 100, Taiwan
[b] Department of Chemistry, National Chung Hsing University, No. 250, Kuo-Kuang Road, Taichung 402, Taiwan
[c] Department of Otolaryngology, National Taiwan University Hospital and College of Medicine, #7, Chung-Shan South Road, Taipei 100, Taiwan
[d] Department of Oncology, National Taiwan University Hospital and College of Medicine, No. 7, Chung-Shan South Road, Taipei 100, Taiwan

ARTICLE INFO

Article history:
Received 22 December 2008
Received in revised form
9 July 2009
Accepted 14 July 2009
Available online 22 July 2009

Keywords:
Photodynamic therapy
Cancer
Synthesis
Asymmetric porphyrins
Mitochondria
Partition coefficients

ABSTRACT

A series of asymmetric porphyrins with varying substituents, such as 4-hydrophenyl and *N*-methyl-4-pyridyl, were synthesized and characterized and their cell uptake, intracellular localization, cytotoxicities and phototoxicities were evaluated in vitro. The most phototoxic of the porphyrins synthesized, 5,10-di-(*N*-methyl-4-pyridyl)-15,20-(4-hydroxyphenyl)-21,23H-porphyrin, which was mainly localized in the mitochondria and displayed low levels of dark toxicity toward human cancer HeLa cells, offers potential application in photodynamic therapy.

1. Introduction

Photodynamic therapy (PDT) is an effective single modality treatment for several medical indications, including cancer, age-related maculopathy, periodontitis, malignant, and pre-malignant skin disorders [1–3]. PDT involves the uptake of the photosensitizing compound (photosensitizer) by cancerous tissues or other sites of therapeutic interest (e.g. neovascular regions), followed by selective irradiation with visible or IR light of an appropriate wavelength that is absorbed by the photosensitizer [4–6]. The advantages of PDT are that it is a precisely targeted treatment that utilizes selective illumination that can be repeated in the same site if necessary, and it is less invasive than surgery. Despite significant advantages, biodistribution of photosensitizers is limited. In addition phototoxicity to the skin, due mainly to the hydrophobicity and non-selectivity of PSs, is another considerable limitation [7].

Three fundamental requirements for PDT are oxygen, light source, and photosensitizer. Each factor is harmless by itself, but their combination can produce cytotoxic agents. In PDT, the photosensitizer preferentially localizes in rapidly growing cells and gets activated by the exposure of light in presence of oxygen to generate reactive oxidative species such as singlet oxygen (O_2^*) as well as other ROS to kill tumor cells [8]. Due to its short lifetime, singlet oxygen intracellular diffusion distance is not more than 0.01–0.02 μm and therefore its direct action is limited to the intracellular structure where the sensitizer localizes [9,10]. Moreover, it is now recognized that damage to certain subcellular structures is correlated with a specific cell death mechanism.

An ideal photosensitizer should have selectivity to tumor cells so as to provide a basis for selectively killing tumor cell. Mitochondrial localized photosensitizers are able to induce apoptosis very rapidly [11] and cytochrome c release is one of the best-known apoptotic events after photosensitization [12,13]. The mitochondrion, due to its pivotal role in arbitrating cell apoptosis [14–16], has recently been considered as a novel pharmacological target for various clinical applications including cancer therapy [17,18]. Mitochondrial dysfunction leads not only to the interruption of the energy supply, but also to the activation of the mitochondria mediated apoptotic pathway [19].

* Corresponding author at: Institute of Biomedical Engineering, College of Medicine and College of Engineering, National Taiwan University, No. 1, Section 1, Jen-Ai Road, Taipei 100, Taiwan. Tel.: +886 2 23123456x81444; fax: +886 2 23912749.
E-mail address: soloman@ntu.edu.tw (M.-J. Shieh).

0143-7208/$ – see front matter © 2009 Elsevier Ltd. All rights reserved.
doi:10.1016/j.dyepig.2009.07.008

Since the first approval of hematoporphyrin derivative (HpD) as a photosensitizer for PDT clinical applications [20], a large number of porphyrin derivatives have been synthesized and investigated for application in PDT; these include *meso*-tetraarylporphyrins, porphyrin dendrimers, core modified porphyrins, chlorins, bacteriochlorins, and phthalocyanines [21–23].

At present there exists no clear correlation between the meso-substituents of porphyrins and their selective accumulation and phototoxicity in tumor cells. Nevertheless, subcellular localization plays a major role in photodynamic efficacy. The cellular affinity of a photosensitizer is governed by its amphiphilic character, which is dependent on the regiochemical arrangement of hydrophobic and hydrophilic meso-substituents in the structure. In this study, we investigated how modifications in the meso-substitution pattern would affect the properties of photosensitizers and tried to develop a novel mitochondria-specific photosensitizer for selective tumor cell killing. This work describes the synthesis of a series of meso-substituted porphyrins (Fig. 1), 4-hydrophenyl, and *N*-methyl-4-pyridyl 4-pyridyl, with varying degrees of hydrophobic/hydrophilic substitutions as model compounds for localization studies of photosensitizers and photodynamic activity in a human carcinoma cell line. Although 5,10,15,20-Tetrakis-(*N*-methyl-4-pyridyl)-21,23H-porphyrin (Porphyrin **1**) and 5,10,15,20-Tetrakis-(4-hydroxyphenyl)-21,23H-porphyrin (Porphyrin **5**) are well known compounds for photodynamic therapy [24,25], Porphyrins **2**, **3**, and **4** have not, hitherto, been shown to display selective accumulation and phototoxicity in tumor cells.

2. Experimental

2.1. Materials and instruments

All reagent grade solvents, including methanol, ethanol, n-hexane, dichloromethane (DCM), acetone, dimethyl sulfoxide (DMSO), and tetrahydrofuran (THF) were obtained from Tedia Inc. (Fairfield, OH, USA), and were dried before application. DCM and THF were dried over CaH_2 and distilled before use. 1,3-diphenylisobenzofuran (DPBF), *n*-octanol, pyrrole, 4-hydroxybenzaldehyde, pyridine-4-aldehyde (caution: irritant; forms explosive mixtures with air at ambient temperatures), 3-(4,5-dimethylthiazol-2-yl)-2,5-diphenyl tetrazolium bromide (MTT), propionic acid and other chemicals were obtained from Aldrich (Milwaukee, WI, USA). ^{1}H NMR spectra were recorded on a Brucker Avance-500 MHz FT-NMR. HRMS were recorded on a Finnigan/Thermo Quest MAT 95XL mass spectrometers. UV/Vis and fluorescence spectra were recorded on a Varian Cary 50 UV–vis Spectrophotometer and Varian Eclipse spectrophotometer respectively.

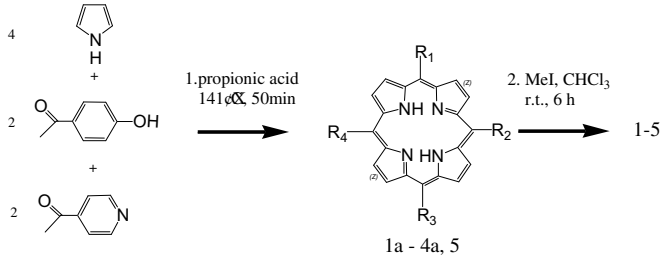

Fig. 1. Synthesis of meso-substituted porphyrin analogues **1**–**5**.

2.2. Synthesis of meso-substituted Porphyrins ***1*–*5***

The synthetic method used in our study was the Adler-Longo method [26]. Adler and Longo modified the Rothemund reaction by allowing benzaldehyde and pyrrole to react for 50 min in refluxing propionic acid (141 °C) in the presence of air. These comparatively mild reaction conditions allowed a wider selection of substituted benzaldehydes to be converted to the corresponding porphyrins in yields of up to about 5%. The reaction was also amenable to large-scale syntheses and multigram quantities of many porphyrins have been prepared.

General Procedure:

Freshly distilled pyrrole (5.6 mL, 0.08 mol), 4-hydroxybenzaldehyde (4.9 g, 0.04 mol), and pyridine-4-aldehyde (3.8 mL, 0.04 mol) were mixed and then refluxing reagent grade propionic acid (200 ml) was added (Fig. 1). After refluxing for 50 min, the solution was cooled to room temperature and filtered, and the filter was washed thoroughly with water. After washing, the resulting purple crystals were air dried, and finally dried *in vacuo* to remove adsorbed acid.

The purification of the products was achieved by repeated column chromatography on silica gel (0.04–0.063 mm, 230–400 mesh ASTM) using dichloromethane, *n*-hexane, and methanol (20:10:1) as eluents. The order of porphyrins eluted down from the column was according to the following sequence 1a, 2a, 3a, 3a-isomer, 4a and then 5. The structural formulas of all compounds are shown in Fig. 1. Methylation was then effected by mixing the precursors with MeI in $CHCl_3$ at room temperature and monitored by TLC, which afforded the target compounds in quantitative yields (>90%). The solvent was removed under reduced pressure and the solid was obtained after washing with diethyl ether. All compounds were characterized by UV, ^{1}H NMR spectroscopy, and Mass spectrometry.

2.2.1. 5,10,15,20-Tetrakis-(N-*methyl-4-pyridyl*)-21,23H-*porphyrin* (***1***)

^{1}H NMR (300 MHz, ppm; dmso-d_6): 9.45 (6H, d, *o*-py), 9.14 (8H, s, β-pyrrole), 8.95 (8H, d, *m*-py), 4.70 (12H, s, CH_3), −3.10 (2H, s, R-pyrrole NH). UV/VIS λ_{max} (H_2O) [nm] (log ε): 419 (5.19), 517 (4.10), 552 (3.83), 585 (3.83), 646 (3.49). MS m/z 1203.6 (M^+–4I) (1202.49 calculated for $C_{44}H_{42}I_4N_8$); found C 44.95, H 3.52, I 42.21, N 9.32.

2.2.2. 5-(4-Hydroxyphenyl)-10,15,20-tri-(N-*methyl-4-pyridyl*)-21,23H-*porphyrin* (***2***)

^{1}H NMR (300 MHz, ppm; dmso-d_6): 9.44 (6H, d, *o*-py), 9.14 (8H, s, β-pyrrole), 8.93 (6H, d, *m*-py), 8.08 (2H, d, OH-phenyl-H*o*), 7.21 (2 H, d, OH-phenyl-H*m*), 4.70 (9H, s, CH_3), −3.11 (2H, s, R-pyrrole NH). UV/VIS λ_{max} (H_2O) [nm] (log ε): 424 (5.17), 521 (3.79), 561 (3.31), 586 (3.30), 646 (2.97). MS m/z 1076.86 (M^+–3I) (1075.56 calculated for $C_{45}H_{40}I_3N_7O$); found C 50.25, H 3.75, I 35.40, N 9.12, O 1.49.

2.2.3. 5,10-Di-(N-*methyl-4-pyridyl*)-15,20-(4-hydroxyphenyl)-21,23H-*porphyrin* (***3***)

^{1}H NMR (300 MHz, ppm; dmso-d_6): 9.45 (4H, d, *o*-py), 9.15 (8H, s, β-pyrrole), 8.95 (4H, d, *m*-py), 8.08 (4H, d, OH-phenyl-H*o*), 7.21 (4 H, d, OH-phenyl-H*m*), 4.70 (6H, s, CH_3), −3.10 (2H, s, R-pyrrole NH). UV/VIS λ_{max} (H_2O) [nm] (log ε): 426 (5.29), 523 (3.94), 566 (3.63), 593 (3.51), 655 (3.33). MS m/z 935.23 (M^+–2I) (932.59 calculated for $C_{44}H_{34}I_2N_6O_2$); found C 56.67, H 3.67, I 27.22, N 9.01, O 3.43.

2.2.4. 5-(N-*Methyl-4-pyridyl*)-10,15,20-tri-(4-hydroxyphenyl)-21,23H-*porphyrin* (***4***)

^{1}H NMR (300 MHz, ppm; dmso-d_6): 9.45 (2H, d, *o*-py), 9.15 (8H, s, β-pyrrole), 8.95 (2H, d, *m*-py), 8.09 (6H, d, OH-phenyl-H*o*), 7.23 (6 H, d, OH-phenyl-H*m*), 4.70 (3H, s, CH_3), −3.09 (2H, s, R-pyrrole NH).

UV/VIS λ_{max} (H_2O) [nm] (log ε): 423 (4.89), 518 (4.63), 553 (3.32), 595 (2.45), 648 (2.86). MS m/z 803.5 (M^+–I) (805.66 calculated for $C_{44}H_{32}IN_5O3$); found C 65.59, H 4.00, I 15.75, N 8.69, O 5.96.

*2.2.5. 5,10,15,20-Tetrakis-(4-hydroxyphenyl)-21,23H-porphyrin (**5**)*

^{1}H NMR (300 MHz, ppm; dmso-d_6): 9.15 (8H, s, β-pyrrole), 8.09 (8H, d, OH-phenyl-H*o*), 7.23 (8 H, d, OH-phenyl-H*m*), −3.10 (2H, s, R-pyrrole NH). UV/VIS λ_{max} (THF) [nm] (log ε): 417 (5.55), 512 (4.24), 551 (4.04) 590 (3.88) 643 (3.53). MS m/z 668.5 (M^+-I) (**678.73** calculated for $C_{44}H_{30}N_4O_4$); found C 77.86, H 4.46, N 8.25, O 9.43.

2.3. Partition coefficients

Lipophilic and hydrophilic properties were characterized by the partition coefficient $P_{o/w} = C_o/C_w$ of each compound between two immiscible solvents *n*-octanol (o) and water (w) [27]. Partition coefficients were determined by adding 20 μM of sensitizer to 5 ml octanol and then adding an equal volume of water. After each phase was presaturated with the other, the tubes were vortexed for 1 min at high speed, placed in a shaker for 4 h at room temperature, and then centrifuged for 10 min at approximately 500 *g* to separate the octanol and water phases. The phase containing the larger quantity of partitioned compound (octanol) was determined and the partition coefficient *P* was characterized.

2.4. Singlet oxygen quantum yields

To evaluate the photosensitizing efficacy of the porphyrins, the singlet oxygen quantum yields (Φ_Δ) were measured by a steady-state method using 1,3-diphenylisobenzofuran as the scavenger [28]. In this procedure a solution of sensitizer and the 1,3-diphenylisobenzofuran singlet oxygen acceptor was illuminated by a light waveband centered at 652 nm which was absorbed only by the sensitizer. The rate of consumption of 1,3-diphenylisobenzofuran was followed spectrophotometrically (Varian Cary 50 UV–Vis spectrophotometer) by observing the decrease of an absorption band at 410 nm as a function of irradiation time. Tetra (4-hydroxyphenyl) porphyrin (p-THPP, $\Phi_\Delta = 0.56$ in methanol) was used as the standard for the determination of absolute quantum yields [29]. In order to improve the accuracy in comparing the quantum efficiencies of the sensitizers, each sensitizer was evaluated under similar experimental conditions. In general, 2.5 mL of methanol containing 1.0 μL of acetic acid was added to adequate amount of sensitizer to give an optical density of 1.00 ± 0.02 at its Soret band. An aliquot of freshly prepared 1,3-diphenylisobenzofuran in acetonitrile (~25 μL) was added to give an optical density = 1.00 ± 0.02 at 410 nm. This solution was illuminated by a 652 nm biolitec PDT laser ($\lambda_{max} = 652$ nm).

2.5. Cell culture and incubation conditions

Human cervical epithelioid carcinoma cells (HeLa) were maintained in a humidified 5% CO_2 incubator at 37 °C in MEM (Gibco BRL, USA) supplemented with 10% heat-activated fetal bovine serum (FBS) and 1% antibiotics (Antibiotic–Antimycotic, Gibco BRL, USA). When cells were in the exponential growth phase, the medium was removed and washed twice with PBS, and then cells were replaced with fresh medium. Procedure to subculture HeLa cells 2–3 times every week.

2.6. Cellular uptake

HeLa cells were seeded on 96-well culture plates at 3000 cells per wells in a 100 μL culture medium. After growing overnight, cells were exposed to various concentrations (0.8–100 μM) of different porphyrins in medium to probe dose-dependent drug accumulation. After incubation for 24 h, the cells were washed with PBS and solubilized in 100 μL of 0.25% Triton X-100 in PBS. The cellular uptake of porphyrins was measured by determining the fluorescence emission of the accumulated porphyrins with Multiwell Fluorscence Plate Reader (Millipore CytoFluor 2300) using excitation/emission wavelengths of Soret band and 670 nm, respectively.

2.7. Cytotoxicity and phototoxicity of porphyrins

To assess the cytotoxicity of the porphyrins, HeLa cells were seeded on a 96-well culture plate at 3000 cells per well in a 100 μL culture medium. The cells were allowed to settle and attached for 24 h. For dark cytotoxicity experiments, porphyrins were added to triplicate wells in 5-fold serial dilutions ranging from 100 μM to 0.8 μM and incubated for 24 h. Phototoxicity experiments were performed with HeLa cells in 96-well plates as described above, with porphyrin concentrations of 100, 50, 20, 4, 0.8, and 0 μM respectively. After 24 h incubation, the compounds were removed, the cells washed with PBS and then exposed to light from LumiSource® (peak wavelength 435 nm, 13.5 mW/cm^2) for 200 s. The total light dose was 1.4 J/cm^2. Cell survival was measured by MTT assay. At 24 h post irradiation, 100 μL of MTT (final concentration 0.5 mg/ml) was added to each well and incubated for 4 h at 37 °C. Then the culture medium was replaced with 100 ul/well DMSO to dissolve the blue formazan crystals produced by mitochondrial hydrogenases in the living cells. The 96-well culture plate was shaken for 15 min at room temperature and read for optical density (OD) immediately at 570 nm on a 318MC ELISA reader (Sanke Instrument Co). The cell survival was expressed by the absorbance changes, and the survival rate was given as the percent ratio of absorbance of treated cells vs. control cells.

2.8. Intracellular localization of porphyrins

Cells were grown on glass slides in 35 mm petri dishes and incubated for 24 h with porphyrins. Cells were washed with PBS and examined directly or after co staining with 100 nM MitoTracker Green FM (M-7514, Molecular Probes Inc, Eugene, OR) for 45 min at 37 °C. Cells were examined with a Leica-SP2 laser scanning confocal microscope (LSCM) (Leica Microsystems Heidelberg GmbH, Heidelberg, Germany). Excitation light was 488 nm for all probes. Fluorescence of the organelle probes was detected with an emission filter of 510–550 nm and porphyrins fluorescence was detected with an emission filter of 640–660 nm.

2.9. Statistical analysis

Mean standard deviation and graphs were used to describe the data. All p values were two-sided and their significance level was 0.05. SPSS 11.0 was used to conduct all statistical analysis.

3. Results

3.1. Chemical characterization of several asymmetric porphyrins

3.1.1. Singlet oxygen quantum yields (Φ_Δ)

It was found that all the compounds were excellent singlet oxygen generators with quantum yield (Φ_Δ) values ranging from 0.25 to 0.64 in methanol (Table 1). Porphyrin **2** displayed the highest quantum yield for singlet oxygen generation (0.64), compared to the other porphyrin derivatives.

Table 1
Photophysical properties of meso-substituted porphyrins.

No.	Compound R1 ~ R4	Absorption λ_{max} in nm (log ε)					Fluorescence λ_{max} (nm)[a]		Singlet oxygen quantum yields (Φ_Δ)[b]	Partition coefficients (log P)
		B (0,0)	*Qy* (1,0)	*Qy* (0,0)	*Qx* (0,1)	*Qx* (0,0)	Q (0,0)	Q (0,1)		
In MeOH PyM:PhOH[c]										
1	4:0	418 (4.39)	527 (3.45)	558 (3.18)	629 (3.28)	690 (3.36)	654	718	0.25	- 1.99
2	3:1	426 (4.87)	522 (3.90)	556 (3.75)	592 (3.66)	652 (3.44)	652	718	0.64	- 0.61
3	2:2	423 (5.15)	519 (4.05)	558 (3.85)	592 (3.71)	651 (4.51)	656	720	0.44	0.53
4	1:3	418 (54.8)	516 (3.69)	550 (3.28)	591 (2.55)	650 (2.76)	656	718	0.45	0.87
5	0:4	417 (5.55)	512 (4.24)	551 (4.04)	590 (3.88)	643 (3.53)	606	658	0.56	1.29
In H_2O PyM:PhOH[c]										
1	4:0	419 (5.19)	517 (4.10)	552 (3.83)	585 (3.83)	646 (3.49)	656	706	0.25	- 1.99
2	3:1	424 (5.17)	521 (3.79)	561 (3.31)	586 (3.30)	646 (2.97)	664	710	0.64	- 0.61
3	2:2	426 (5.29)	523 (3.94)	566 (3.63)	593 (3.51)	655 (3.33)	662	708	0.44	0.53
4	1:3	423 (4.89)	518 (4.63)	553 (3.32)	595 (2.45)	648 (2.86)	654	716	0.45	0.87
5	0:4	434 (4.91)	526 (2.99)	564 (3.88)	607 (3.26)		654	718	0.56	1.29

[a] Excited at soret band.
[b] Using Tetra (4-hydroxyphenyl) porphyrins (p-THPP, Φ_Δ=0.56 in methanol) as the reference.
[c] PyM and PhOH are presented as *N*-methyl-4-pyridyl and hydroxyphenyl, respectively.

3.1.2. Partition coefficient

The degrees of lipophilicities of meso-substituted porphyrins were determined by the partition coefficient values between octanol and aqueous phase (Table 1). The porphyrins with greater number of *N*-methyl-4-pyridyl substituents exhibited higher hydrophilicity. However, the degrees of lipophilicities of meso-substituted porphyrins increased as the number of 4-hydrophenyl-substitutents increased.

3.1.3. Absorbance and emission spectra

The fluorescence emission and UV–visible spectral data of these porphyrins in THF and H_2O are shown in Fig. 2. The fluorescence maxima show two bands (654–720 nm) upon the excitation by Soret bands. Their UV–visible spectra consist of the intense Soret band around 418–434 nm and weaker Q bands in the 510–660 nm intervals with difference extinction coefficients in different solvent (Table 1).

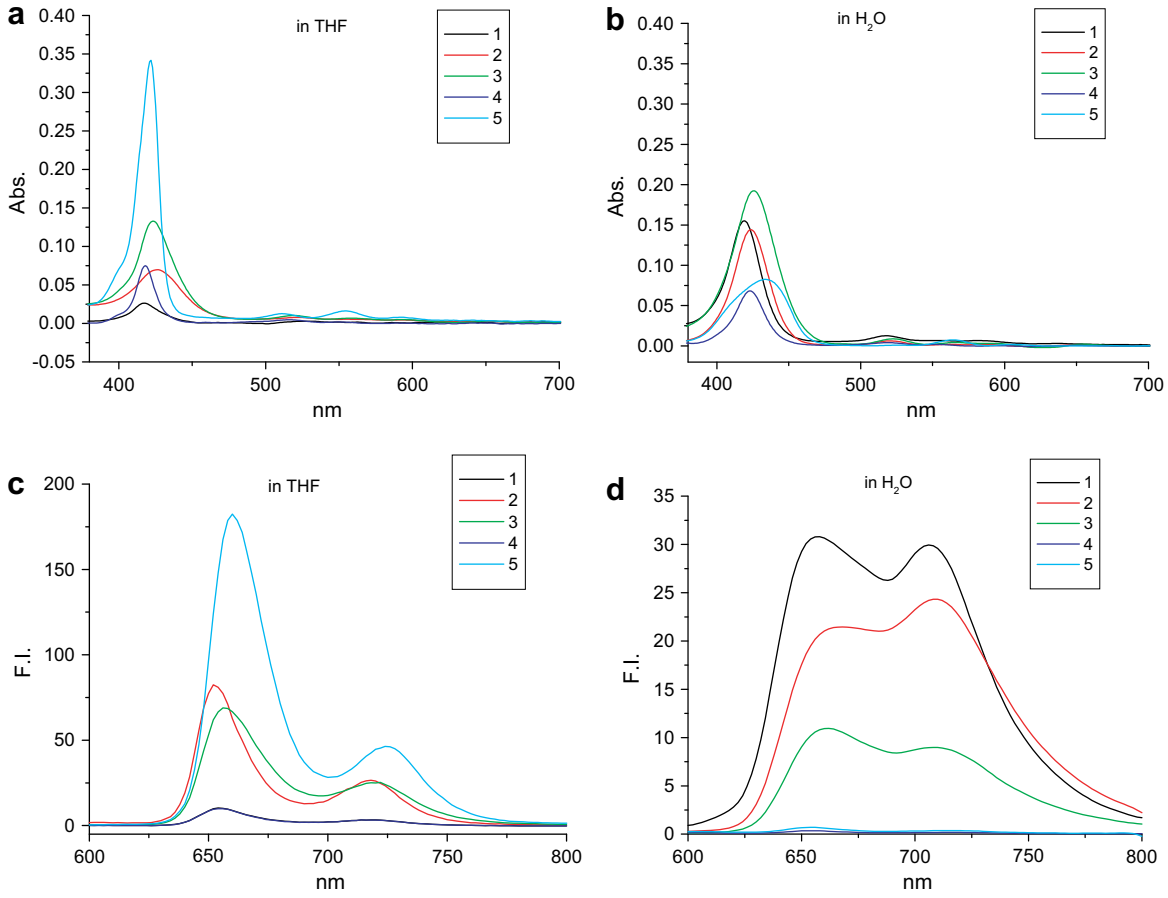

Fig. 2. UV–vis absorbance spectra of porphyrin derivatives **1**–**5** (1 μM) in THF (a) and in H_2O (b) Emission spectra of cationic porphyrin derivatives **1**–**5** (1 μM) in THF (c) and in H_2O (d). (λ_{ex} = soret band).

3.2. In vitro studies

3.2.1. Cellular uptake of porphyrins

The cellular uptake was investigated in HeLa cells incubated in the medium with the different porphyrin derivatives **1**–**5** respectively for 24 h. Under similar conditions, the Porphyrins **2**, **4**, and **5** exhibited the highest uptake, and Porphyrin **1** had the lowest uptake at either high or low concentration (Fig. 3). The uptake of porphyrin derivatives were in the order of **5** = **4** = **2** > **3** > **1** at high concentration (20 μM). Compared to the partition coefficients of porphyrin derivatives (Fig. 3), their cellular uptake increased proportionately with their corresponding partition coefficients ($\log p$). The porphyrins with lower partition coefficient had a lower cellular uptake by the HeLa cells.

3.2.2. Cytotoxicity and phototoxicity of porphyrins

The concentration-dependent dark cytotoxicity was investigated in HeLa cells exposed to each porphyrin with different concentrations (up to 100 μM) for 24 h in the dark. The dark cytotoxicity of porphyrin derivatives increased proportionately with the increase in porphyrin concentration. Porphyrins **5** and **4** showed higher dark cytotoxicity levels, whereas Porphyrin **1** exhibited a lower dark cytotoxicity value (Fig. 4). Porphyrins **5** and **4** showed a higher dark cytotoxicity probably as a result of the higher cell uptake. The cytotoxicity of porphyrin derivatives seemed to follow the partition coefficient values in the order of **5** > **4** > **2** > **3** > **1** (Fig. 3 vs. Fig. 4).

However, those porphyrins were found to be phototoxic toward human HeLa cells, upon exposure to low light dose (1.4 J/cm^2), as shown in Fig. 4(b). Lower concentrations of porphyrin derivatives were also found to have a pronounced effect on cell viability. Porphyrin **3** was the most phototoxic and the LD_{90} (light treatment that results in a 90% cell kill) was about 3.1 μM, followed by Porphyrin **5** (LD_{90} ~ 4.9 μM) Porphyrin **4** (LD_{90} ~ 6.9 μM), Porphyrin **2** (LD_{90} ~ 20 μM), and Porphyrin **1** (LD_{90} > 50 μM). Although Porphyrin **2** exhibited the highest singlet oxygen quantum yield of this series of porphyrins in MeOH, its phototoxicity was lower than that of the other porphyrins. Porphyrins with high hydrophilicity cannot easily diffuse across the cell membrane and consequently have a lower cellular uptake. It was demonstrated that Porphyrin 1 showed low levels of cell uptake resulting in a lower cytotoxicity value and photodynamic efficiency.

The high phototoxicity of Porphyrin **3** despite its low cellular uptake and relatively low singlet oxygen generating efficiency

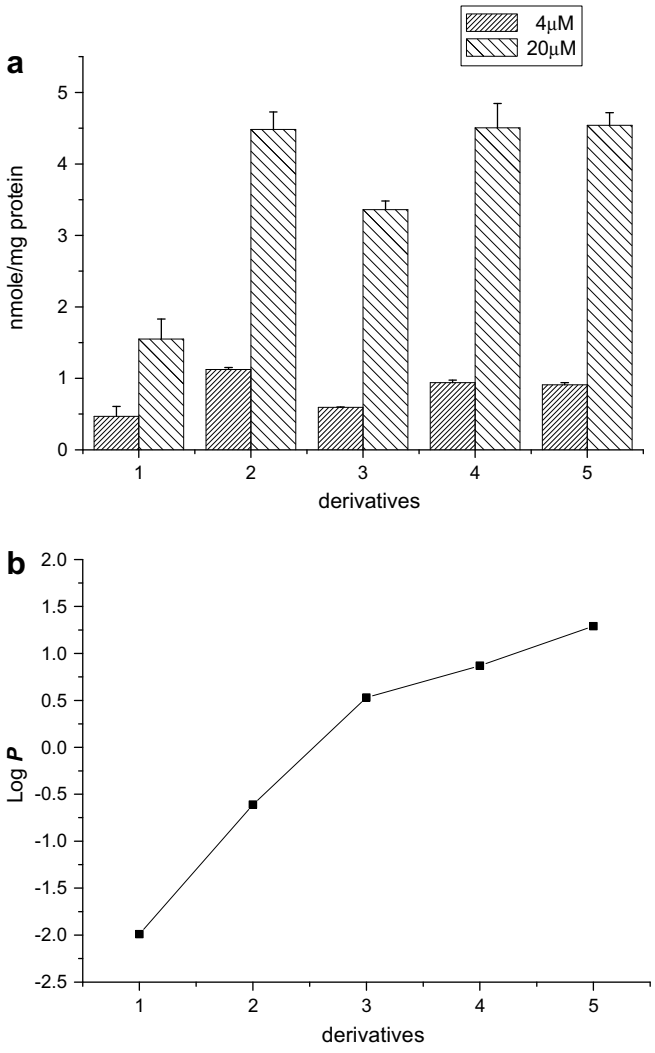

Fig. 3. Comparison of cellular uptake (a) and partition coefficient (b) of a series of porphyrin derivatives **1**–**5** at 4 and 20 μM for 24 h by HeLa cell.

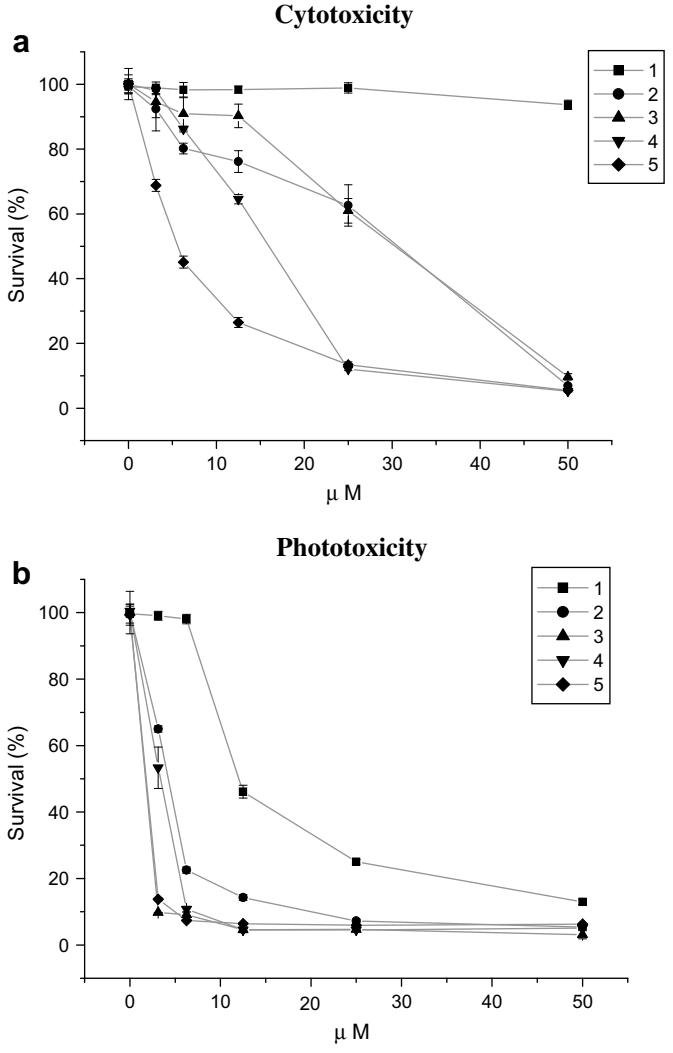

Fig. 4. (a) Drug dose-response curves obtained in HeLa cells following exposure to different porphyrin derivatives for 24 h; and (b) irradiation with blue light (LumiSource®, 7 mW/cm^2) for 200 s (1.4 J/cm^2). The colorimetric MTT test was used for cell death estimation.

could be explained by its specificity for mitochondrial localization (Fig. 5). These results show that the degree of phototoxicity of porphyrin derivatives correlates not only with their the ability for generating singlet oxygen or the extent of their uptake into cells but also on their specificity of subcellular localization.

3.2.3. Intracellular localization of porphyrins

In a comparative study with MitoTracker Green, the different porphyrins showed distinct localizations in mitochondria. A representative localization pattern of the most effective Porphyrins (**3**–**5**) and the most ineffective Porphyrins (**1** and **2**) are shown in Fig. 5.

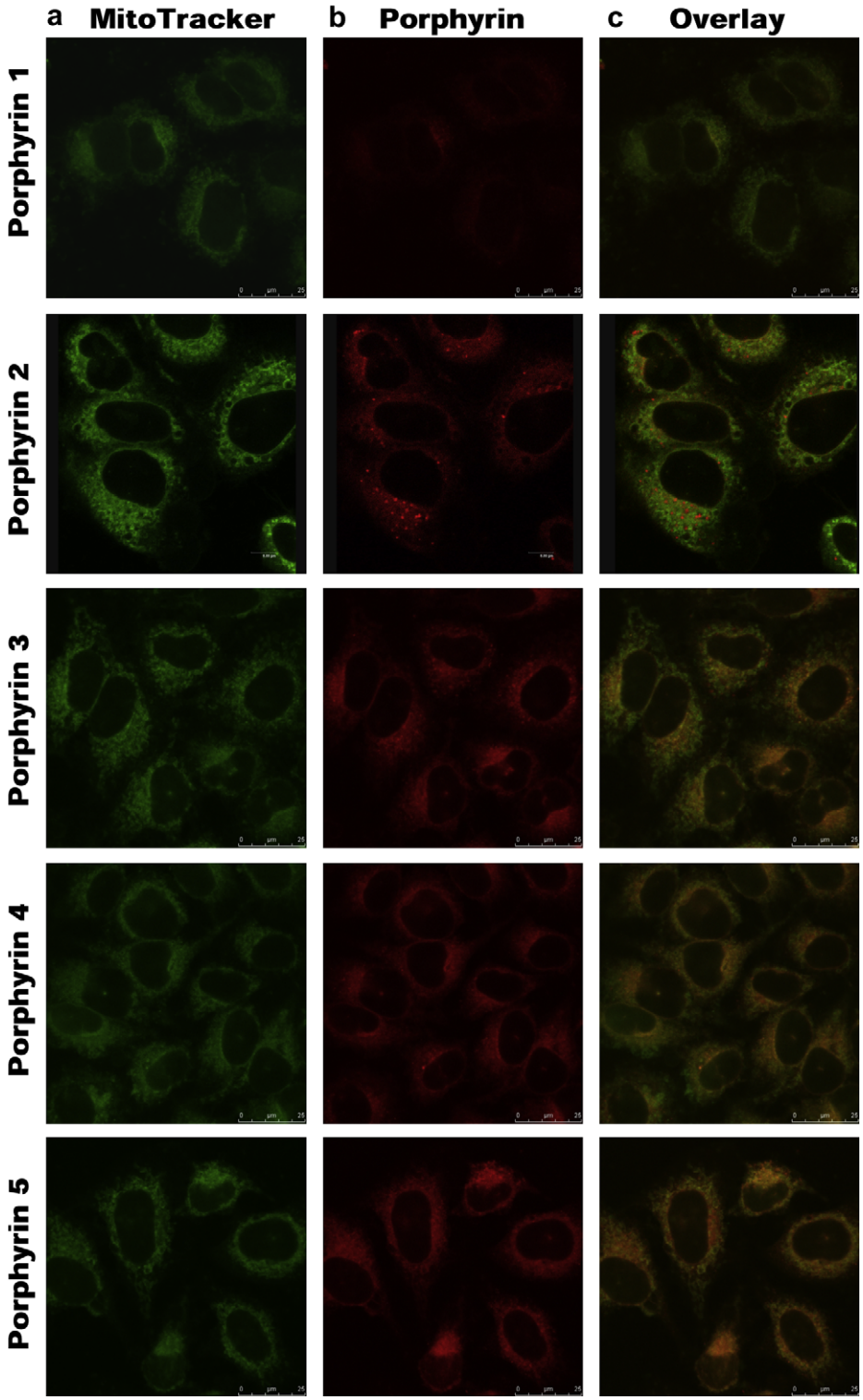

Fig. 5. Subcellular localization of porphyrin derivatives **1**–**5** in HeLa cells at 10 μM for 24 h. (a) MitoTracker Green fluorescence (b) porphyrin fluorescence (c) overlays of MitoTrackers with porphyrin fluorescence.

Porphyrins **3**–**5** were found to localize in mitochondria, whereas Porphyrin **2** had less colocalization with MitoTracker Green. Porphyrin **2** ($LD_{90} \sim 20\ \mu M$) and was less effective in vitro PDT, even though its cellular uptake and ability for generating singlet oxygen were high. As the result of confocal imaging, Porphyrin **2** exhibited more aggregation in the cytosol, and Porphyrin **1** showed a low fluorescence intensity due to its higher hydrophilicity and consequently for its lower extent of cell uptake.

4. Discussion

An ideal photosensitizer should act on novel cellular targets that are specific for cancer cells and sufficiently different from normal cells so as to provide a basis for selective tumor cell killing. The cellular affinity of a photosensitizer is governed by its amphiphilic character, which is dependent on the regiochemical arrangement of meso-substituents in the structure. In this study, we investigated how the modification in the meso-substitution pattern would affect the properties of porphyrin photosensitizers with the goal of developing a novel mitochondria-specific photosensitizer for selective tumor cell killing.

Amphiphilicity is also important because it can affect cellular uptake and the degree to which the photosensitizer aggregates, which, in turn, can affect its photophysical properties [30]. It is well known that the photophysical properties of tetrapyrrole photosensitizer (PS) are strongly affected by their aggregation state [20]. It is also generally accepted that aggregated PS are less photoactive, *i.e.*, they are less fluorescent, generate less singlet oxygen in solution, and produce less triplet-state PS as determined by laser flash photolysis [31]. Comparing the partition coefficient values of porphyrin derivatives (Table 1), we found best cellular uptake and photodynamic efficiency occurred with a partition coefficient ($\log p$) ranging from about 0.55 to 1.29 in this series of porphyrin derivatives.

A photosensitizer's structure, charge and overall lipophilicity determine how it interacts with itself and its surroundings, which also influence the site of localization in cells [32]. Margaron et al.[33] and others [34] have reported that amphiphilic photosensitizers are generally more photodynamically active than symmetrically hydrophilic or hydrophobic molecules. Besides, too high partition coefficient may let the porphyrin aggregate in the culture medium, as a consequence, decreasing its cellular uptake. However, the porphyrin with high hydrophilicity cannot easily diffuse across the cell membrane. It was demonstrated that Porphyrin **1** showed low level of cell uptake explaining its low cytotoxicity and low photodynamic efficiency.

Obviously Porphyrins **3**–**5** were found to localize in mitochondria, whereas Porphyrins **1**–**2** had less colocalization with MitoTracker Green. Some reports confirmed that the aggregation state of intracellular photosensitizes affect their localization, with the more aggregated species tending toward lysosomal localization [35–37]. In this series, Porphyrin **2** with the higher degree of aggregation was the less active photosensitizing agent, whereas Porphyrin **3** that localized in the mitochondria was more effective in in vitro PDT despite its low cellular uptake. Determination of the target site of the photosensitizer binding has long been a goal of PDT research [38]. It has been shown that effective photosensitizers have very diverse patterns of localization, and it seems to be based on structure, lipophilicity, charge, and amphiphilicity. The site of drug localization appears to be an important factor for photodynamic efficiency, in addition to cellular uptake.

5. Conclusions

In summary, many key factors such as lipophilicity, asymmetric structure and subcellular localization of photosensitizers play a key role in their cellular uptake and photocytotoxicity. In our study, 5,10-di-(*N*-methyl-4-pyridyl)-15,20-(4-hydroxyphenyl)-21,23H-porphyrin (Porphyrin **3**) showed a higher phototoxicity probably due to its more specific mitochondrial localization, even though its cellular uptake and singlet oxygen generating efficiency were not the best in the series of porphyrin derivatives synthesized. Based on the results of our study, this organelle-selective porphyrin can be used as a basis for the synthesis of more compounds with improved specificity and potency for potential anti-tumor therapy in the future.

Acknowledgements

This research was supported by grants from National Science Council of the Republic of China (NSC 97-2120-M-002-017).

References

[1] Harrod-Kim P. Tumor ablation with photodynamic therapy: introduction to mechanism and clinical applications. Journal of Vascular and Interventional Radiology 2006 Sep;17(9):1441–8.
[2] Lai PS, Lou PJ, Peng CL, Pai CL, Yen WN, Huang MY, et al. Doxorubicin delivery by polyamidoamine dendrimer conjugation and photochemical internalization for cancer therapy. Journal of Controlled Release 2007;122(1):39–46.
[3] Prosst RL, Wolfsen HC, Gahlen J. Photodynamic therapy for esophageal diseases: a clinical update. Endoscopy 2003;35(12):1059–68.
[4] Kennedy JC, Pottier RH, Pross DC. Photodynamic therapy with endogenous protoporphyrin. 9. Basic principles and present clinical-experience. Journal of Photochemistry and Photobiology B – Biology 1990;6(1–2):143–8.
[5] Spikes JD. Porphyrins and related compounds as photodynamic sensitizers. Annals of the New York Academy of Sciences 1975;244(APR15):496–508.
[6] Ochsner M. Photophysical and photobiological processes in the photodynamic therapy of tumours. Journal of Photochemistry and Photobiology B – Biology 1997;39(1):1–18.
[7] Zhang GD, Harada A, Nishiyama N, Jiang DL, Koyama H, Aida T, et al. Polyion complex micelles entrapping cationic dendrimer porphyrin: effective photosensitizer for photodynamic therapy of cancer. In: 11th International symposium on recent advances in drug delivery systems and CRS winter symposium; 2003 Mar 03–06. Salt Lake City, Utah: Elsevier Science Bv; 2003. p. 141–50.
[8] Dougherty TJ, Gomer CJ, Henderson BW, Jori G, Kessel D, Korbelik M, et al. Photodynamic therapy. Journal of the National Cancer Institute 1998;90(12):889–905.
[9] Shieh MJ, Peng CL, Lou PJ, Chiu CH, Tsai TY, Hsu CY, et al. Non-toxic photo-triggered gene transfection by PAMAM-porphyrin conjugates. Journal of Controlled Release 2008;129(3):200–6.
[10] Oleinick NL, Evans HH. The photobiology of photodynamic therapy: cellular targets and mechanisms. Radiation Research 1998;15(5):S146–56.
[11] Kessel D, Luo Y. Mitochondrial photodamage and PDT-induced apoptosis. Journal of Photochemistry and Photobiology B – Biology 1998;42(2):89–95.
[12] Morgan J, Oseroff AR. Mitochondria-based photodynamic anti-cancer therapy. Advanced Drug Delivery Reviews 2001;49(1–2):71–86.
[13] Oleinick NL, Morris RL, Belichenko T. The role of apoptosis in response to photodynamic therapy: what, where, why, and how. Photochemical & Photobiological Sciences 2002;1(1):1–21.
[14] Yang J, Liu XS, Bhalla K, Kim CN, Ibrado AM, Cai JY, et al. Prevention of apoptosis by Bcl-2: release of cytochrome c from mitochondria blocked. Science 1997;275(5303):1129–32.
[15] Liu XS, Kim CN, Yang J, Jemmerson R, Wang XD. Induction of apoptotic program in cell-free extracts: requirement for dATP and cytochrome c. Cell 1996;86(1):147–57.
[16] Jou MJ, Jou SB, Chen HM, Lin CH, Peng TI. Critical role of mitochondrial reactive oxygen species formation in visible laser irradiation-induced apoptosis in rat brain astrocytes (RBA-1). Journal of Biomedical Science 2002;9(6):507–16.
[17] Szewczyk A, Wojtczak L. Mitochondria as a pharmacological target. Pharmacological Reviews 2002;54(1):101–27.
[18] Modica-Napolitano JS, Kulawiec M, Singh KK. Mitochondria and human cancer. Current Molecular Medicine 2007;7(1):121–31.
[19] Modica-Napolitano JS, Singh KK. Mitochondrial dysfunction in cancer. Elsevier Sci Ltd; 2004. pp. 755–62.
[20] Kessel D. Hematoporphyrin and hpd – photophysics, photochemistry and phototherapy. Photochemistry and Photobiology 1984;39(6):851–9.
[21] Detty MR, Gibson SL, Wagner SJ. Current clinical and preclinical photosensitizers for use in photodynamic therapy. Journal of Medicinal Chemistry 2004;47(16):3897–915.
[22] Brown SB, Brown EA, Walker I. The present and future role of photodynamic therapy in cancer treatment. Lancet Oncology 2004;5(8):497–508.
[23] Huang Z. A review of progress in clinical photodynamic therapy. Technology in Cancer Research & Treatment 2005;4(3):283–93.

[24] Konan YN, Berton M, Gurny R, Allemann E. Enhanced photodynamic activity of meso-tetra(4-hydroxyphenyl)porphyrin by incorporation into sub-200 nm nanoparticles. European Journal of Pharmaceutical Sciences 2003;18(3–4): 241–9.
[25] Colombo LL, Vanzulli SI, Villanueva A, Canete M, Juarranz A, Stockert JC. Long-term regression of the murine mammary adenocarcinoma, LM3, by repeated photodynamic treatments using meso-tetra (4-N-methylpyridinium) porphine. International Journal of Oncology 2005 Oct;27(4):1053–9.
[26] Adler AD, Sklar L, Longo FR, Finarell Jd, Finarell Mg. A mechanistic study of synthesis of meso-tetraphenylporphin. Journal of Heterocyclic Chemistry 1968;5(5):669.
[27] Leo A, Hansch C, Elkins D. Partition coefficients and their uses. Chemical Reviews 1971;71(6):525.
[28] Spiller W, Kliesch H, Wohrle D, Hackbarth S, Roder B, Schnurpfeil G. Singlet oxygen quantum yields of different photosensitizers in polar solvents and micellar solutions. Journal of Porphyrins and Phthalocyanines 1998;2(2):145–58.
[29] Bonnett R, McGarvey DJ, Harriman A, Land EJ, Truscott TG, Winfield UJ. Photophysical properties of meso-tetraphenylporphyrin and some meso-tetra (hydroxyphenyl)porphyrins. Photochemistry and Photobiology 1988;48(3): 271–6.
[30] Smith GJ. The effects of aggregation on the fluorescence and the triplet-state yield of hematoporphyrin. Photochemistry and Photobiology 1985;41(2):123–6.
[31] Redmond RW, Land EJ, Truscott TG. Aggregation effects on the photophysical properties of porphyrins in relation to mechanisms involved in photodynamic therapy. Advances in Experimental Medicine and Biology 1985;193:293–302.
[32] Mason MD. Cellular aspects of photodynamic therapy for cancer. Reviews in Contemporary Pharmacotherapy 1999;10(1):25–37.
[33] Margaron P, Gregoire MJ, Scasnar V, Ali H, vanLier JE. Structure–photodynamic activity relationships of a series of 4-substituted zinc phthalocyanines. Photochemistry and Photobiology 1996;63(2):217–23.
[34] Boyle RW, Dolphin D. Structure and biodistribution relationships of photodynamic sensitizers. Photochemistry and Photobiology 1996;64(3):469–85.
[35] MacDonald IJ, Morgan J, Bellnier DA, Paszkiewicz GM, Whitaker JE, Litchfield DJ, et al. Subcellular localization patterns and their relationship to photodynamic activity of pyropheophorbide-a derivatives. Photochemistry and Photobiology 1999;70(5):789–97.
[36] Trivedi NS, Wang HW, Nieminen AL, Oleinick NL, Izatt JA. Quantitative analysis of Pc 4 localization in mouse lymphoma (LY-R) cells via double-label confocal fluorescence microscopy. Photochemistry and Photobiology 2000;71(5):634–9.
[37] Peng CL, Lai PS, Shieh MJ. Influence of substitutions in asymmetric porphyrins on intracellular uptake, subcellular localization and phototoxicity in Hela cells. Biomedical Engineering-Applications Basis Communications 2008;20(1):9–17.
[38] Kessel D, Luo Y. Photodynamic therapy: a mitochondrial inducer of apoptosis. Cell Death and Differentiation 1999;6(1):28–35.